27
2-1-77
25 cy to NTIS

UCID- 17326

Lawrence Livermore Laboratory

PREDICTING SUBSIDENCE OVER COAL-GASIFICATION SITES

Robert Langland
David Fletcher

November 22, 1976

MASTER

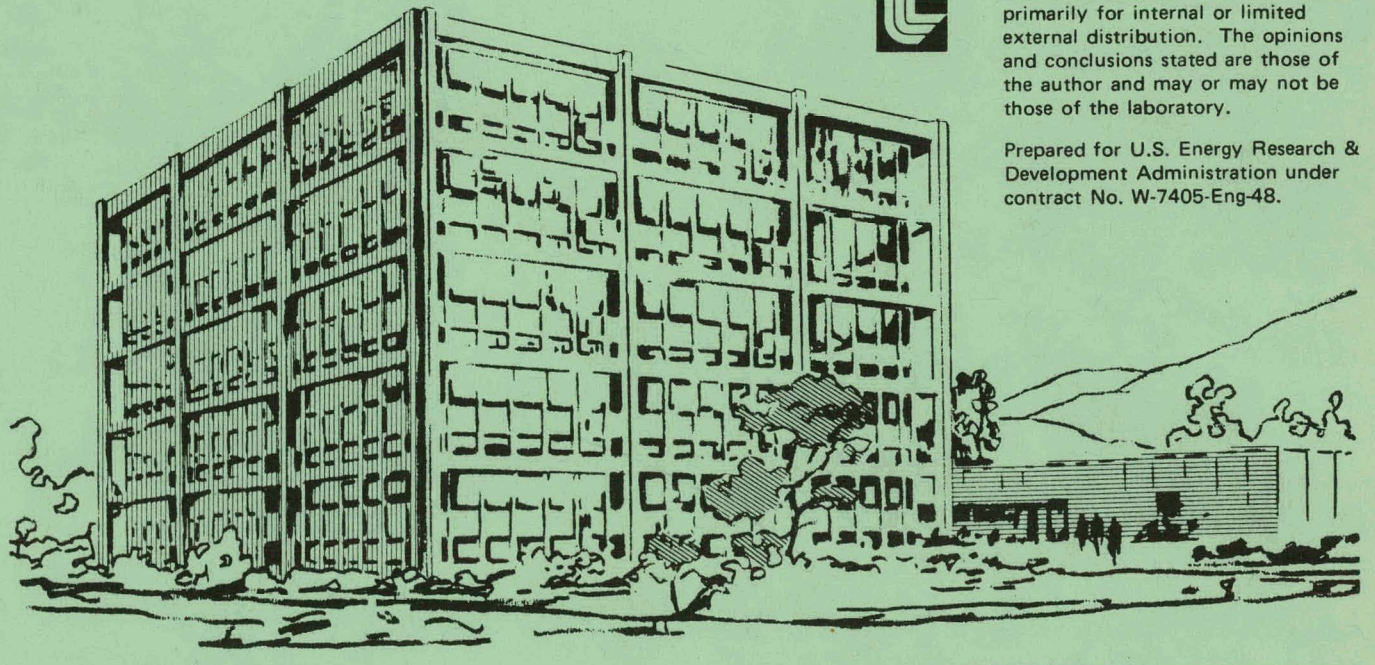

Prepared for U.S. Energy Research & Development Administration under contract No. W-7405-Eng-48.

DISCLAIMER

THIS PAGE

WAS INTENTIONALLY

LEFT BLANK

CONTENTS

PREDICTING SUBSIDENCE OVER COAL-GASIFICATION SITES

ABSTRACT

The extent to which earth subsidence may be caused by *in situ* coal gasification is studied using the method of finite elements. This study takes into account rock failure modes and nonlinearity of rock stiffness. Two models were studied for the site at Hoe Creek, where a coal seam is overlain and underlain by interbedded clays and sandstones. These two studies are expected to bracket any subsidence that may occur. Maximum subsidence was 0.06 in. using the stiff model and 3.5 in. using the soft model, neither of which suggests undesirably large subsidence.

INTRODUCTION

An investigation of surface movement has been undertaken in conjunction with work at LLL to develop a method of *in situ* coal gasification. A priori knowledge of surface strains and displacements can help answer many practical questions about the design of an *in situ* plant, and it can provide information about such a plant's environmental impact.

State-of-the-art predictive techniques employ measurements of actual subsidence over existing cavities whose geometry and geologic surroundings are similar to those of a cavity under consideration. The use of these methods, therefore, is restricted to those areas where considerable previous mining has taken place. We are attempting to find a more general method that can be applied to any excavation, including mining (or other extraction) in virgin areas. The technique chosen uses current structural-analysis procedures (in particular, the finite-element method) to predict surface movement. Previous analyses have had limited success, except in the case of very deep seams.

It is clear that most rock masses have low tensile strength. This inability to carry tension can be an intrinsic property of the solid rock (as it is in concrete, for instance) but it is more likely due to the presence of faults and/or fractures. A routine qualitative estimation of the stresses surrounding an underground opening shows that tensile stresses are to be

expected in the vicinity. Thus, it is evident that tensile failure is possible. A model for rock materials should therefore incorporate some failure mechanism. Theoretically this presents no difficulty, but practically, failure is somewhat difficult to handle. Tensile failure is taken into account in the present analysis by using a material whose modulus of elasticity in tension is two to three orders of magnitude smaller than it is in compression. In addition, an elastic-plastic analysis is also used to allow plastic yielding.

Recent equation-of-state work has shown that many rocks exhibit nonlinear stress-strain behavior. This nonlinearity is difficult to incorporate in practical analyses, and thus it has been largely ignored. The present method provides for nonlinear stress-strain relations and for differences between the loading and unloading/reloading properties of the material. These refinements, in combination with the analytical potential of the finite-element method, provide a general technique for the prediction of surface movement above underground openings.

The method of extraction, *in situ* coal gasification, presents some problems that are not encountered in more conventional mining situations. The geometry of the pilot plants analyzed here shows that the ratio of the coal seam thickness to the opening width is on the order of 0.5, whereas the corresponding ratio for conventional longwall coal mines is less than 0.01. This difference indicates that comparisons of results from analyses of conventional mines with those from analyses of coal gasification plants may not be valid. It is therefore expected that verification of the analytical results can come only from actual measurements of subsidence.

Perhaps the most significant problem to be overcome in developing this analysis is the choice of suitable material properties. It is initially tempting to simply use laboratory properties; however, the sampling and test procedures result in much larger values for moduli than can be reconciled with field behavior. *In situ* testing using geophysical methods also produces high values for moduli, although we feel that the relative values of moduli between various layers may be well represented. The problem is then reduced to one of adjusting the absolute values obtained from the logging to give reasonable values for subsidence. It is assumed that a pragmatic approach should be taken, i.e., the analysis will attempt only to predict subsidence.

ANALYSIS OF THE HOE CREEK SITE

The gasification experiment planned for Hoe Creek is expected to produce a cylindrical cavity approximately 50 ft in diameter in a 25-ft-thick coal seam at a depth of 175 ft. The overburden material consists of interbedded clays and sandstones. The geometry and stratigraphy are shown in Fig. 1. The problem is idealized axisymmetrically to simplify the finite-element analysis. This simplification allows the use of more time steps in the analysis, which will produce a more accurate model of the progression of failure around the cavity.

In addition to the surface movements (U_z), the variation of horizontal displacement (U_r) with depth is of considerable interest. The magnitude of U_r is not as important as the derivative $\partial U_r/\partial Z$, which, when large, indicates a potential for slip displacement and therefore the possibility of damage to the holes and pipes that supply reactant gases or extract product gas.

Another result of the finite-element analysis is information concerning the behavior of subsurface strata. This information is necessary for evaluating possible damage to aquifers that may overlie the coal seam.

MATERIAL MODELS

The overburden rock was modeled using an isotropic, nonlinear elastic material to represent the clastic materials and an isotropic elastic-perfectly plastic material to represent the clay. A von Mises yield criterion was assumed. The presence of a water table at about 60 ft required that five material zones be used. (The final finite-element mesh is shown in Fig. 2.) The various material properties are given in Table 1. In the case of the nonlinear elastic materials, the properties are linear in tension but nonlinear in compression, so both the initial and final tangent moduli are given. The dependence of the compressive moduli on the volume strain (e) is (1) initial compressive loading:

$$K = K_F - (K_F - K_I)\exp(e/c_1) \qquad e < e_{max} \leq 0$$

$$G = G_F - (G_F - G_I)\exp(e/c_2) \qquad e < e_{max} \leq 0 \qquad (1)$$

and (2) repeat compressive loading and unloading:

$$K = \overline{K} + (K_I - \overline{K})\ e/c_1 \qquad e_{max} < e < 0$$

where

$$\overline{K} = \text{lesser of} \begin{cases} K_F - (K_I - K_F)\ e_{max}/c_1 \\ K_I \end{cases}$$

$$G = G_F - (G_F - G_I)\ \exp(e_{max}/c_2)$$

and where the subscripts F and I represent final and initial values, respectively. The constants c_1 and c_2 merely control the rate at which the final tangent moduli are approached with increasing compressive volume strain.

The lack of specific data on the elastic properties of the *in situ* materials creates some uncertainty when modeling the actual site. However, a bounding approach was used to show what would be considered a 'worst case.' Birch gives typical ranges of values for bulk modulus (K) and shear modulus (G) of $12 \times 10^6 < K < 0.8 \times 10^6$ psi and $12 \times 10^6 < G < 0.5 \times 10^6$ psi, respectively.[1] Since these are laboratory values on solid rock, it is appropriate to reduce them by one or two orders of magnitude to more accurately model *in situ* materials.[2] Thus, for the stiff model, the values of K and G for rock were chosen to be 1.25×10^6 psi and 0.38×10^6 psi, respectively (Poisson's ratio = 0.36); for the soft model, the values were 0.125×10^6 psi and 0.038×10^6 psi (see Table 1). It is anticipated that

Table 1. Properties for stiff and soft models. Soft properties are shown in parenthesis.

Material			Density	K_I	K_F	G_I	G_F			K_{tens}	G_{tens}
Type	Description	No.	(ft^{-3})	(10^5 psi)	(10^5 psi)	(10^5 psi)	(10^5 psi)	c_1	c_2	(10^5 psi)	(10^5 psi)
Clay (dry)	elastic-plastic	1	112	1.6 (0.016)	1.6 (0.016)	0.157 (0.00157)	0.157 (0.00157)	–	–	1.6 (0.016)	0.157 (0.00157)
Clastics (dry)	nonlinear elastic	2	135	1.6 (0.16)	12.5 (1.25)	1.25 (0.125)	3.80 (0.38)	0.05 (0.05)	0.006 (0.006)	0.5 (0.05)	0.4 (0.04)
Coal	nonlinear elastic	3	90	0.16 (0.016)	1.25 (0.125)	0.125 (0.0125)	0.380 (0.0380)	0.05 (0.05)	0.006 (0.006)	0.05 (0.05)	0.04 (0.04)
Clay (sat.)	elastic-plastic	4	120	1.6 (0.016)	1.6 (0.016)	0.157 (0.00157)	0.157 (0.00157)	– –	– –	1.6 (0.016)	0.157 (0.00157)
Clastics (sat.)	nonlinear elastic	5	142	1.6 (0.16)	12.5 (1.25)	1.25 (0.125)	3.80 (0.38)	0.05 (0.05)	0.006 (0.006)	0.05 (0.05)	0.04 (0.04)

these choices should bracket the actual material properties and that the subsequent analysis should reflect typical values of surface subsidence.

GEOMETRY AND BOUNDARY CONDITIONS

The finite-element idealization of the area surrounding the opening is shown in Fig. 2. Past experience with subsidence problems indicates that the model should extend laterally to a distance equal to at least 1.5 times the depth to the seam and that the underburden should be of approximately the same thickness as the overburden. These dimensions are desirable to minimize the effects of boundary conditions.

The boundary conditions imposed on the model consist of a free surface on top and conditions of frictionless confinement on the sides and bottom (i.e., $U_r = 0$ on the sides and $U_z = 0$ on the bottom). Thus, the horizontal stresses σ_h in the unexcavated states will be related to the vertical stresses σ_v by the relationship

$$\sigma_h = \frac{\nu}{1 - \nu} \sigma_v$$

where ν is Poisson's ratio.

The opening is developed in three stages by removing the elements shown in the crosshatched area in Fig. 2. It is assumed that no material remains after the burn front passes. It is also assumed that effects from thermally induced strains and internal pressurization can be ignored. This latter assumption merely indicates that the subsidence values obtained will apply to the final state of the gasification opening. The first assumption will produce a conservative estimate, i.e., the predicted degree of subsidence will be larger or equal to the actual subsidence if material is left in the cavity. Previous calculations have shown that if the residual material is only 1/20 as stiff as the original material, no tensile stresses develop in the vicinity of the cavity, and the subsidence is minimal. It is therefore felt that the subsidence predicted by the current analysis will be greater than that measured in the field.

DISCUSSION OF RESULTS

The results of the analyses are shown in Figs. 3 through 13. The graphs are generally in pairs; the first shows the values for the stiff model, and

the second shows those for the soft model. Figures 3 and 4 show the variation with depth of the vertical stress above the center of the opening; the solid line represents the stresses in the unexcavated state, while the dots represent the final stresses after the excavation is complete. The final stresses indicate that the effects of the opening become significant at about 50 to 60 ft above the opening. The degree of stress relief below the opening is shown by the slow return of the vertical stress to the original stress (solid line). The difference at Z = 307 represents the material removed. Figures 5 and 6 show principal stress contours in the final deformed state. The contours clearly depict the redistribution of stresses around the opening. Of particular interest is the development of tensile stresses in the clastic layers above the opening (this effect is more evident in the soft-material analysis). A tensile region also develops in the region of the opening itself. It should be assumed that the materials in the floor and roof, which are in tension, have failed, and consequently, that the opening has been enlarged.

The displacement components are shown in Figs. 7 through 13. Figures 7 and 8 show the surface subsidence profiles for the two analyses. They are typical of observed profiles for continuum analyses, i.e., no discontinuities are present. The magnitudes of maximum subsidence for the two cases are 0.06 in. for the stiff model and 3.5 in. for the soft model. Neither of these values indicates an undesirably large surface movement. As was stated previously, the material in the soft model should be less stiff than the *in situ* material, and therefore the 3.5 in. predicted displacement should be an upper bound on the actual subsidence.

Figures 9 and 10 show the final deformed shape of the material layers. The distortion in the immediate vicinity of the opening is evident. It can also be seen that there is very little surface motion apparent even though the roof of the opening has moved several feet. The relative magnitudes of horizontal displacements can be discerned from these figures as well.

An analysis of the horizontal displacement field is necessary to determine the effects of ground motion on pipes and casings near the opening. Figures 9 and 10 indicate that the maximum horizontal displacement occurs just above the edge of the opening. Figure 11 shows the variation of horizontal displacement with increasing distance from the centerline at a depth of 166 ft. The maximum displacement occurs at R = 20.8 ft. This would indicate the point at which the distortion of pipes or casings would be maximum.

Figures 12 and 13 depict the variation of horizontal displacement with depth along the line R = 20.8 ft; the plot would therefore represent the distorted shape of a pipe in that zone. As expected, the soft model shows the largest displacement, but the quantity of greatest interest is the flexural rotation of the pipe, which is roughly the magnitude of the displacement divided by the length over which the displacement occurs. In the case of the soft model, a displacement of 25 in. occurs over a length of 9 ft (108 in.) for a rotation of 0.23 radians, which is actually very severe. Flexible couplings would seem advisable in the region of the cavity.

CONCLUSIONS

The analyses indicate that surface subsidence at the Hoe Creek site will be minimal (on the order of a few inches). Some difficulty in holding pipes may be experienced, but only when the opening is completed. The presence of residue in the opening is a mitigating factor that would tend to reduce all effects.

The effects of internal pressurization or thermal strains have not been included. These effects will not be present after gasification is completed, which is when subsidense effects are greatest. During production, the existence of gases under pressure in the cavity should reduce tensile stresses and subsidence.

REFERENCES

1. F. Birch, "Elastic Constants of Rocks," in *Handbook of Physical Constants*, S. P. Clark, Jr., Ed. (Geol. Soc. of America, New York, 1966), pp. 160-168.
2. H. D. Dahl and D. S. Choi, "Some Case Studies of Mine Subsidence and its Mathematical Modeling," in *Proc. Fifteenth Symposium of Rock Mechanics, 1973* (South Dakota School of Mines and Technology, Rapid City, 1973).

GPL/af/rm,md/lmc

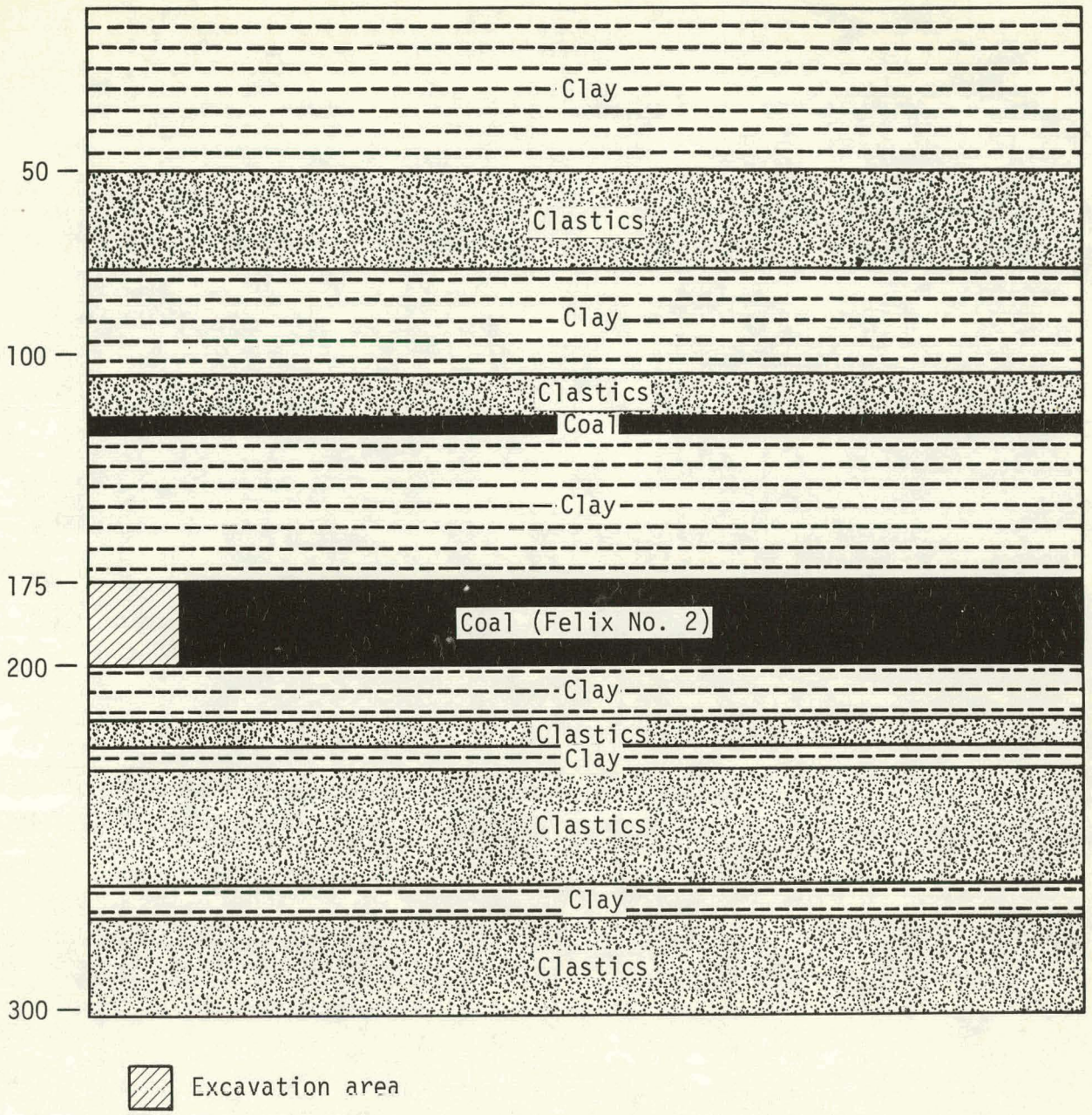

Fig. 1. The stratigraphic column at the Hoe Creek site as modeled.

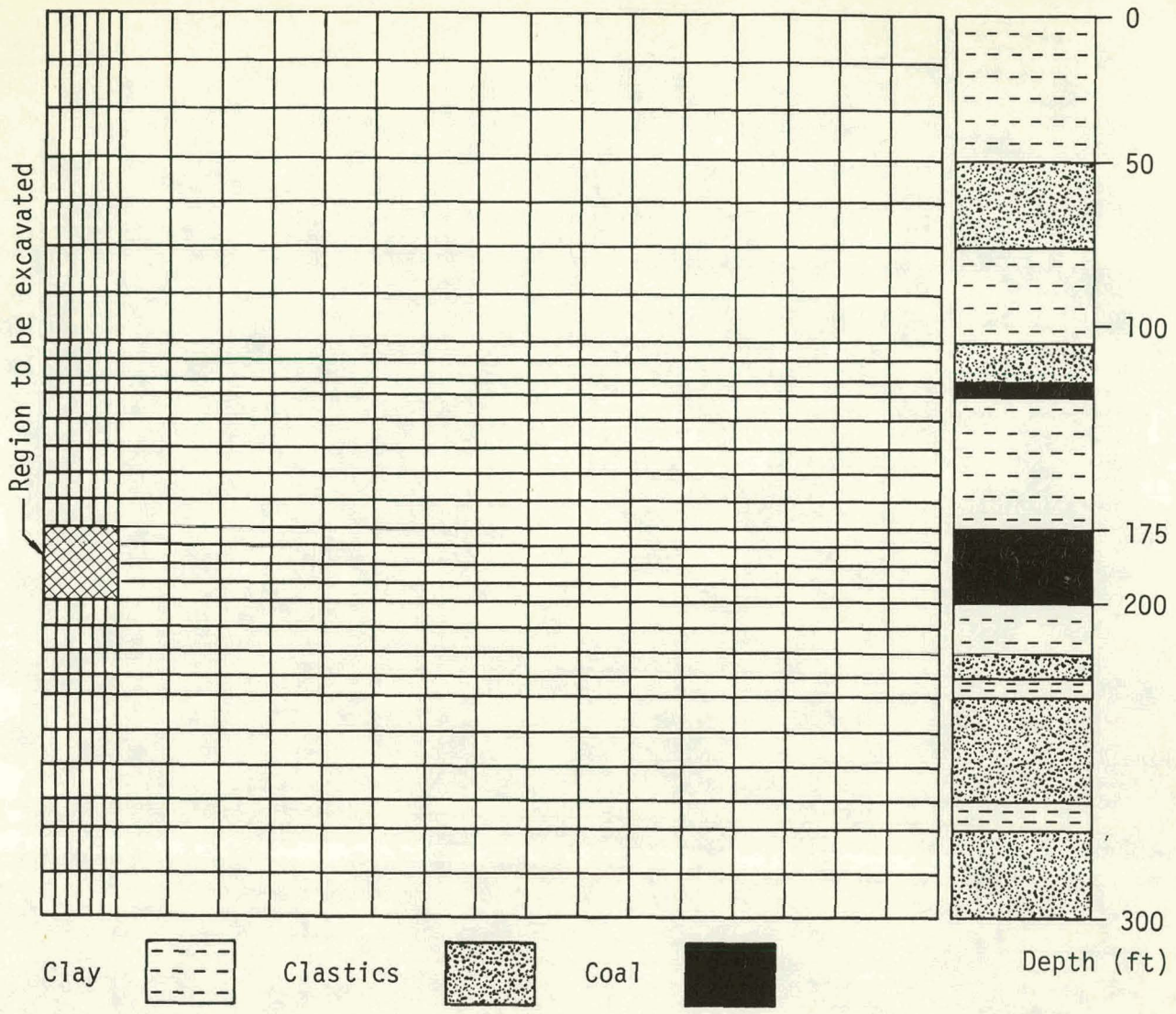

Fig. 2. Plot of the mesh for the final finite-element model.

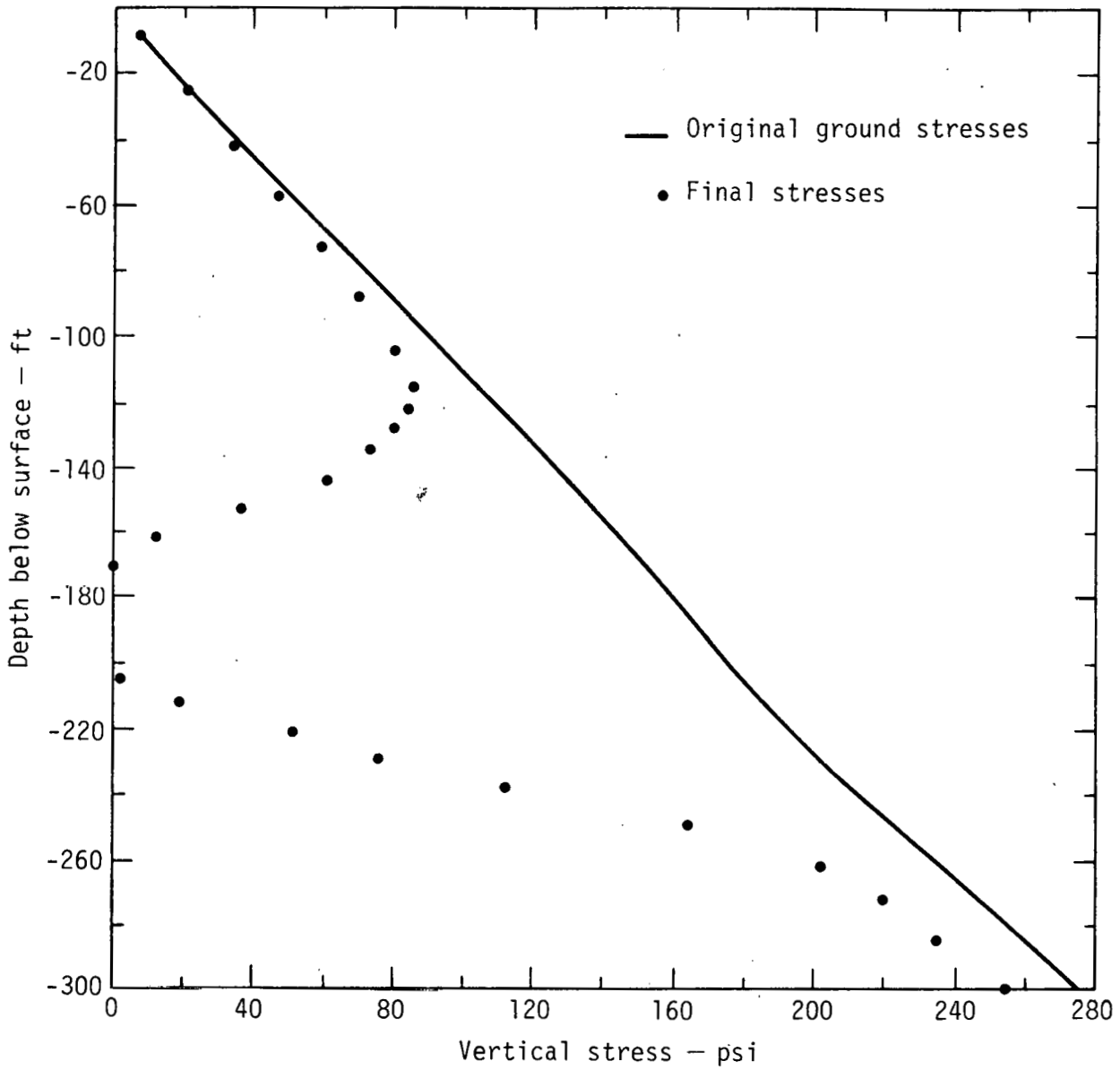

Fig. 3. Vertical stresses along the centerline of the model (stiff material).

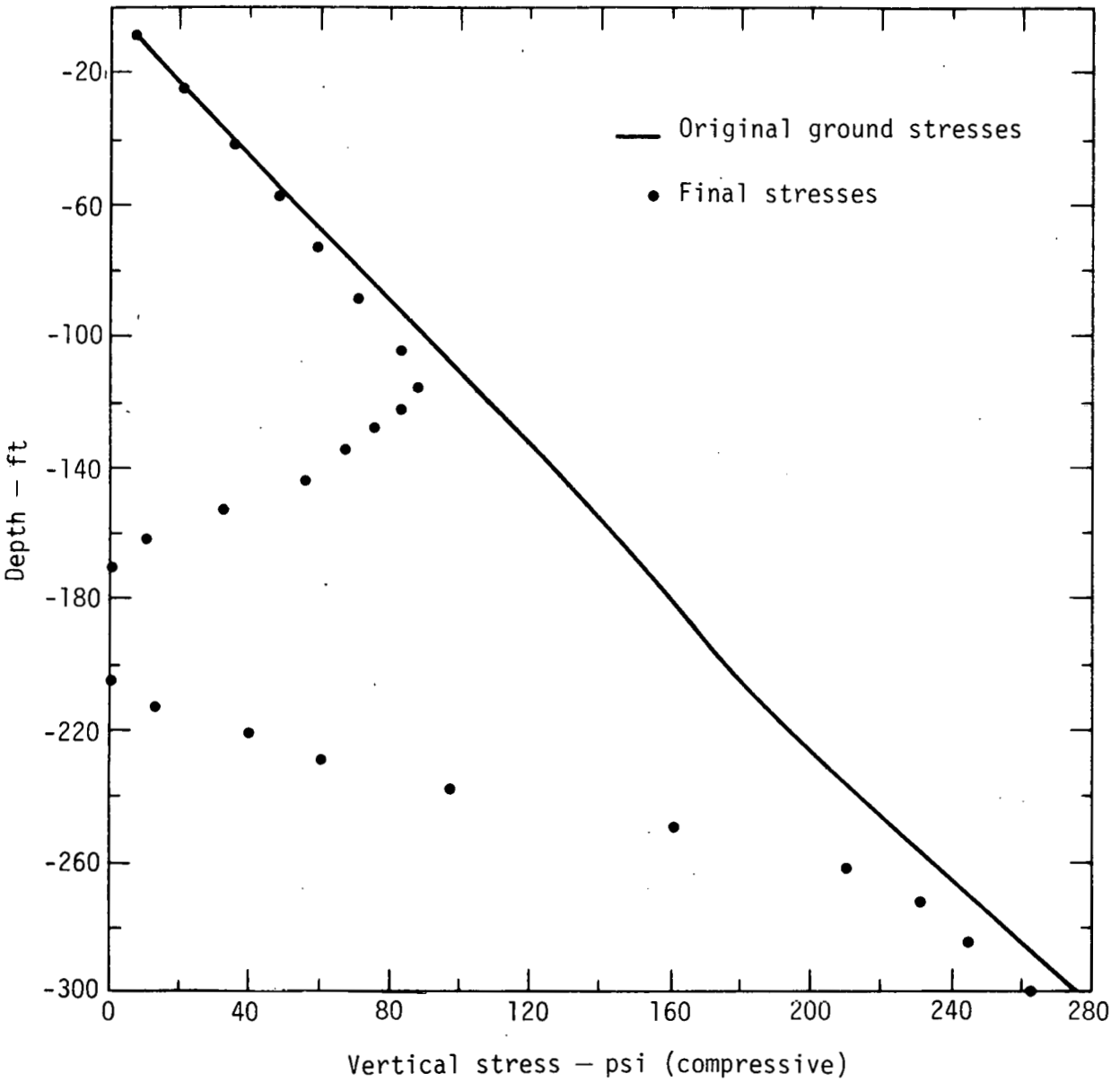

Fig. 4. Vertical stresses along the centerline of the model (soft material).

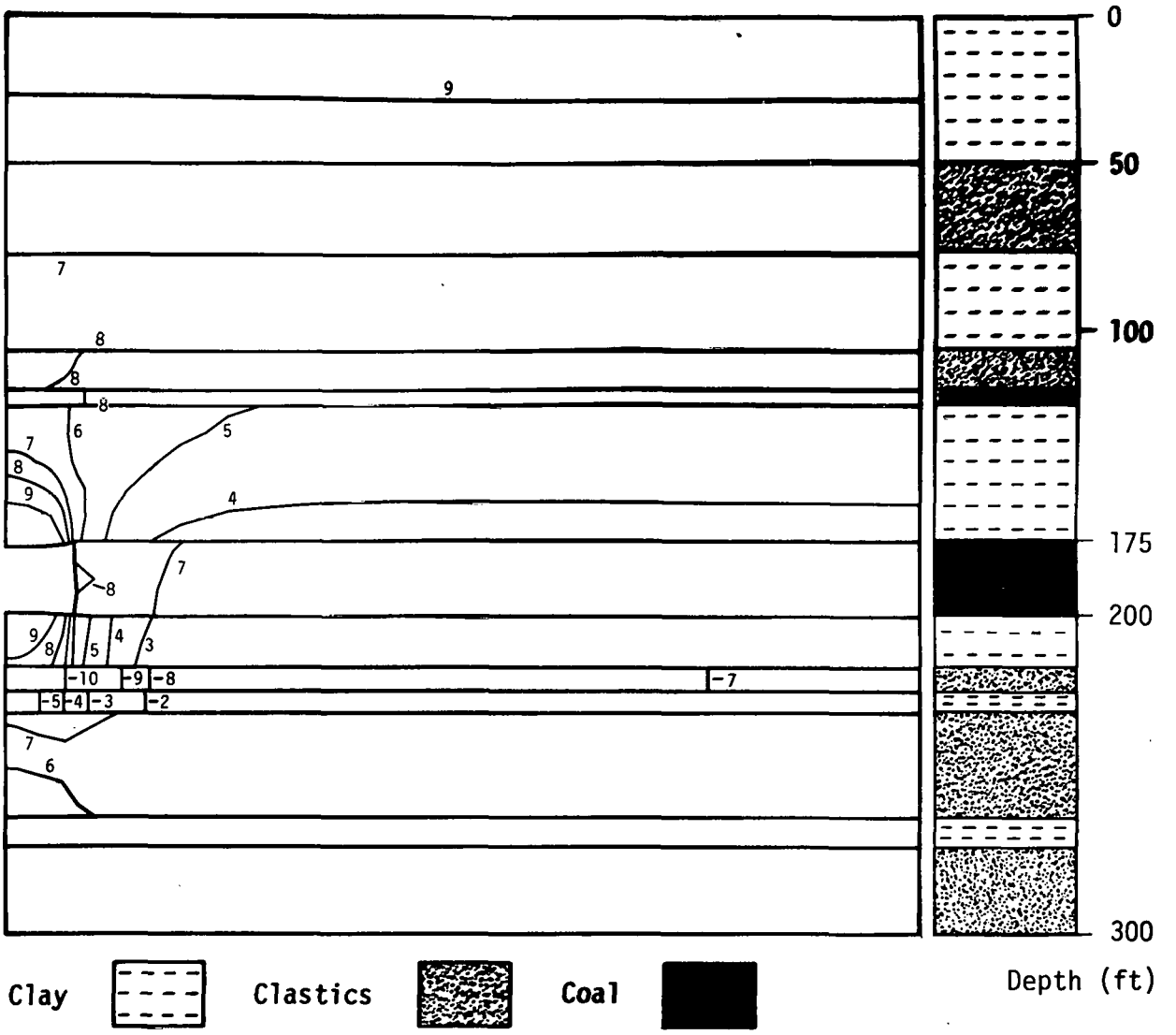

Fig. 5. Contours of the maximum principal stresses for the stiff model (1 = -20 psi, 3 = -61, 5 = -100, 7 = -140, 9 = -180).

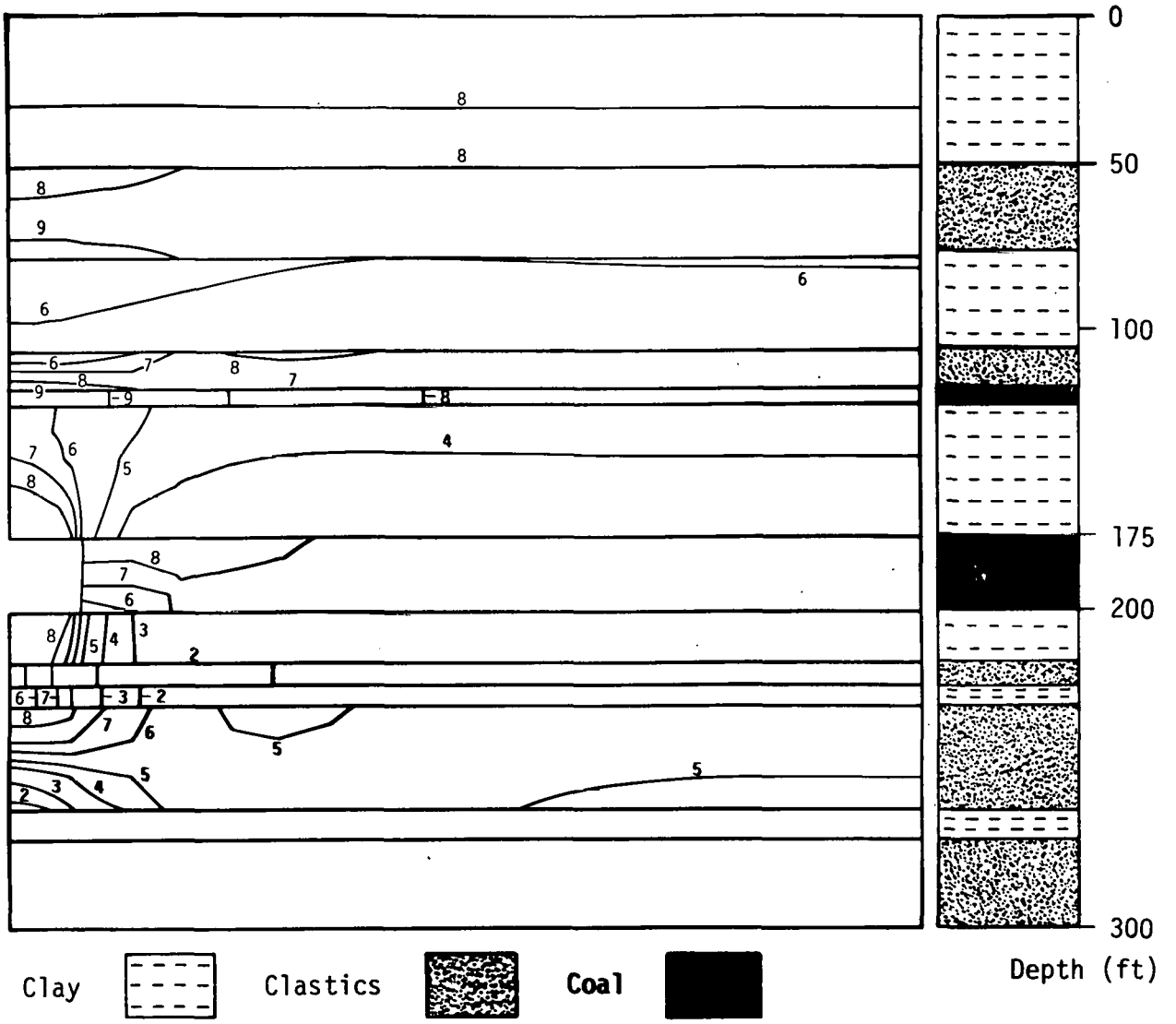

Fig. 6. Contours of the maximum principal stresses for the soft model. (1 = 2 psi, 3 = -44, 5 = -90, 7 = -140, 9 = -180).

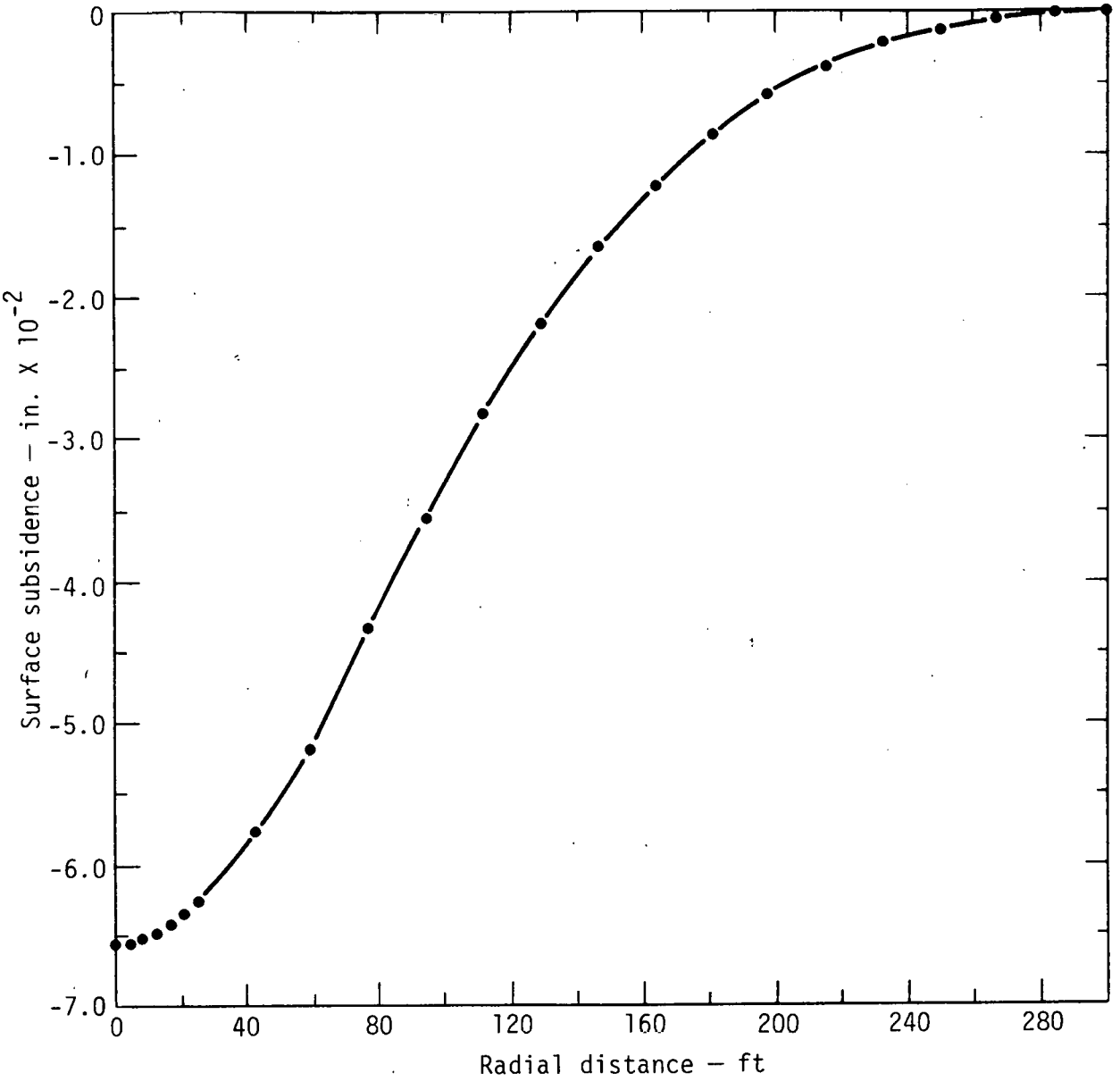

Fig. 7. Surface subsidence profile for the stiff model.

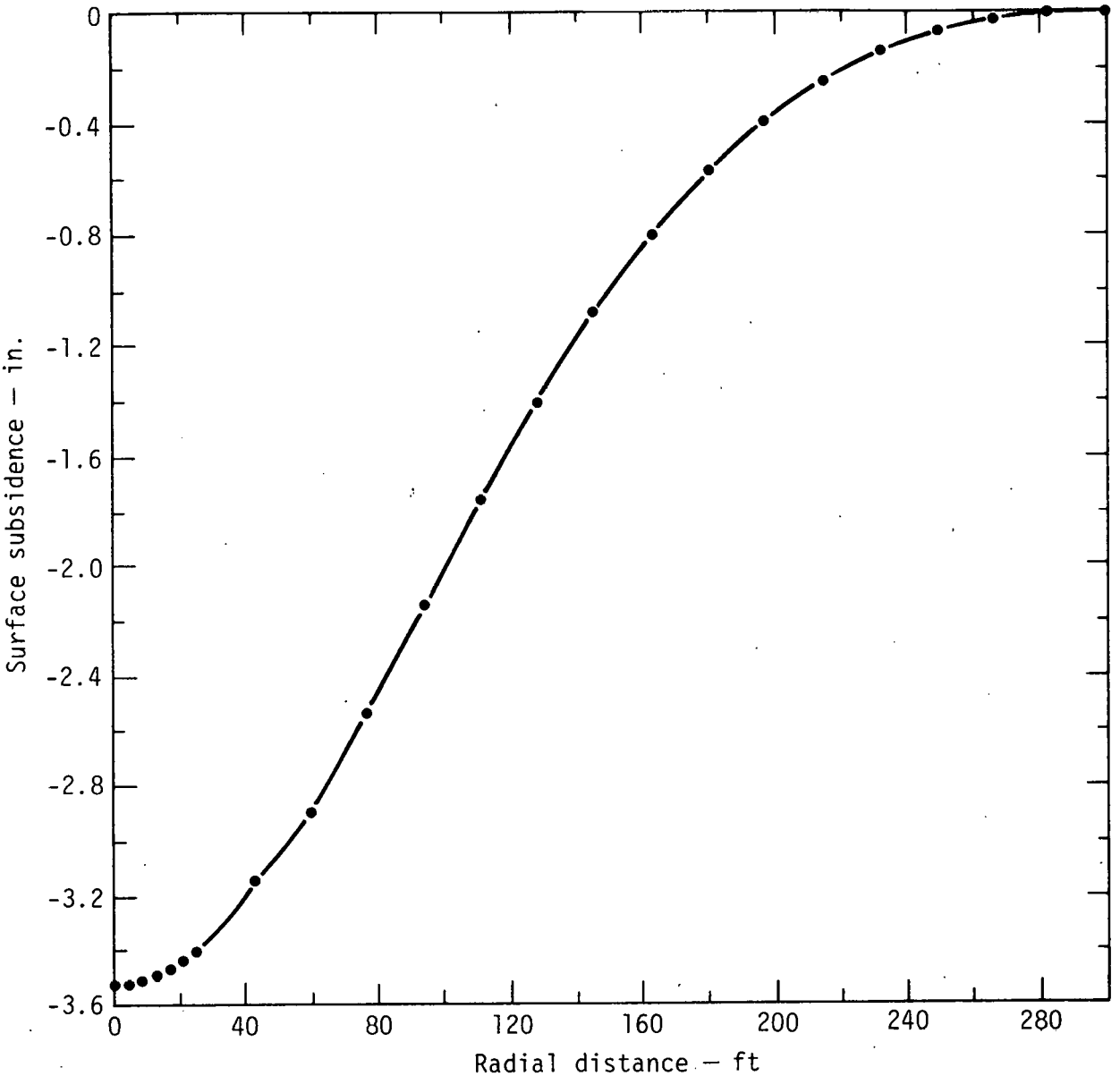

Fig. 8. Surface subsidence profile for the soft model.

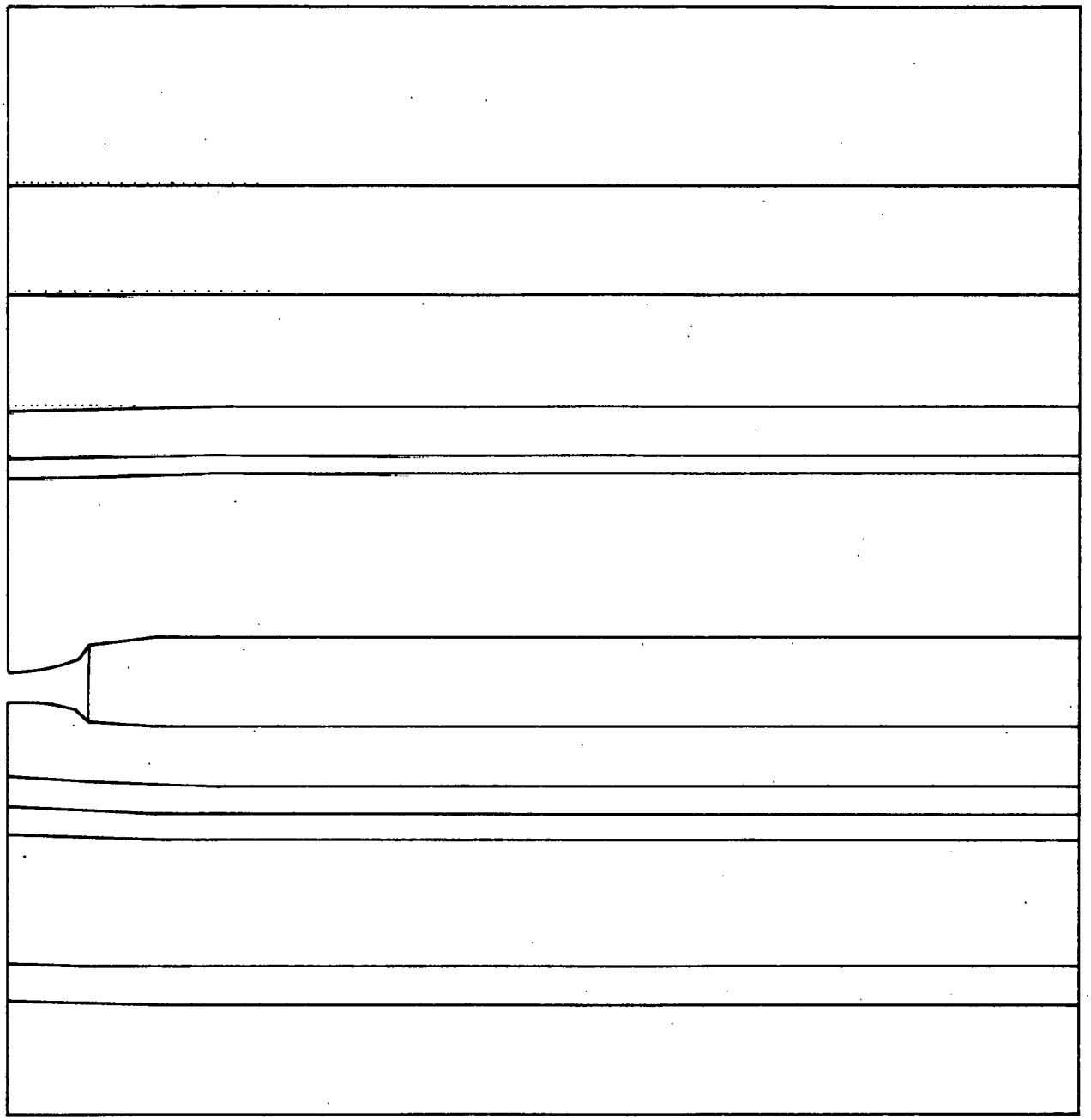

Fig. 9. Deformed mesh for the stiff model (displacements are scaled by a factor of 10).

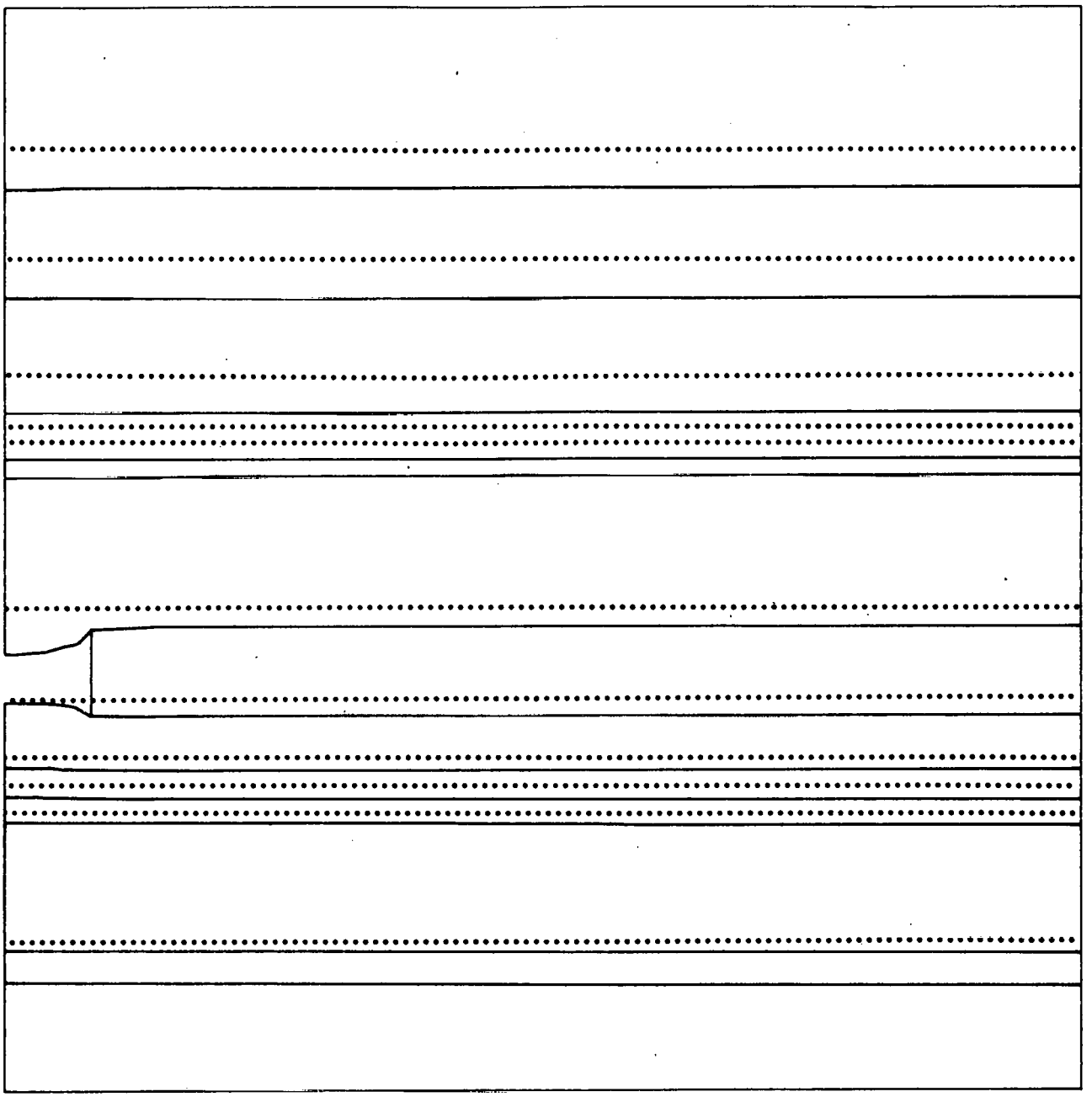

Fig. 10. Deformed mesh for the soft model (displacements are not scaled).

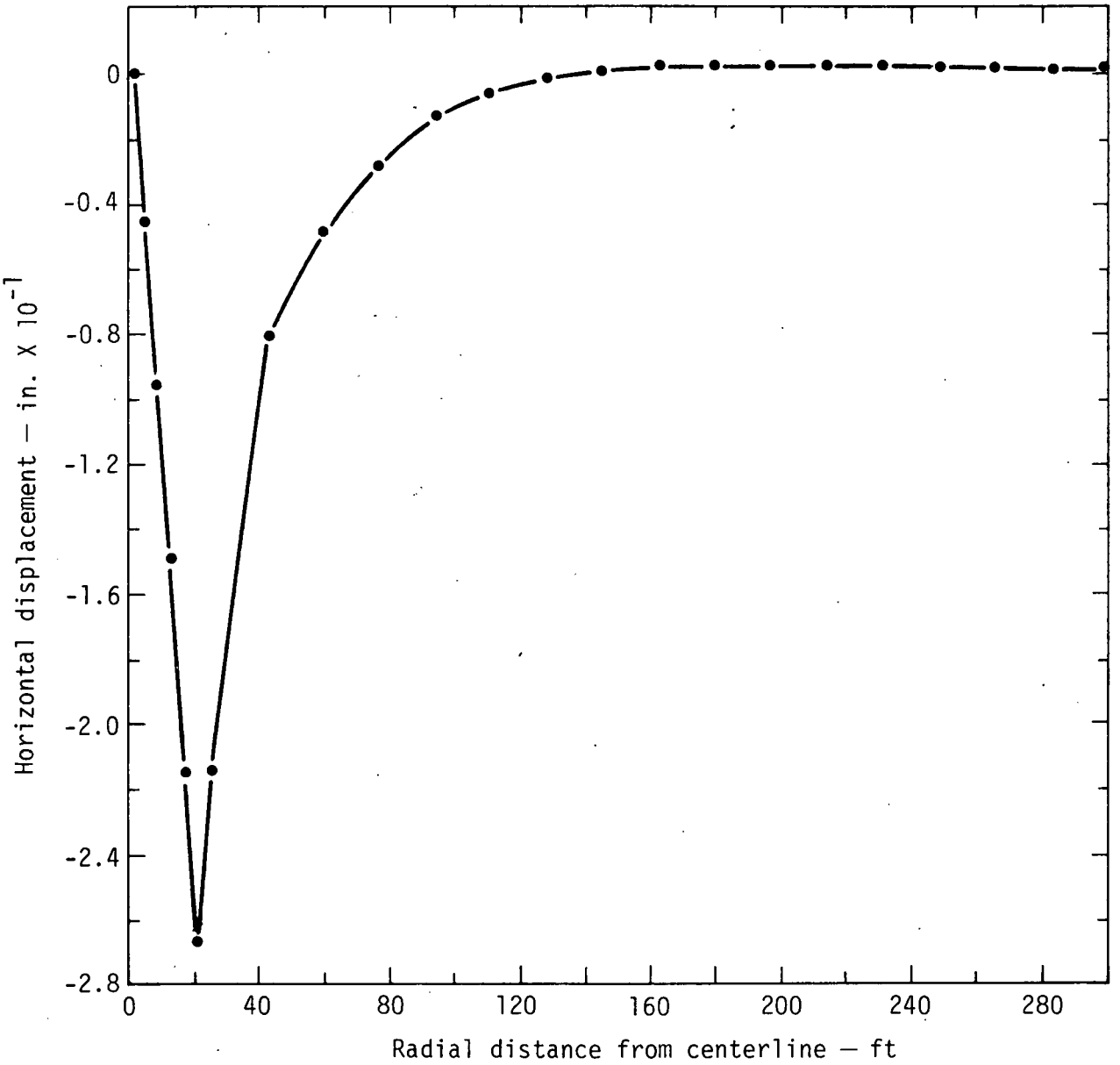

Fig. 11. Horizontal displacement on the plane z = -166 ft for the stiff model.

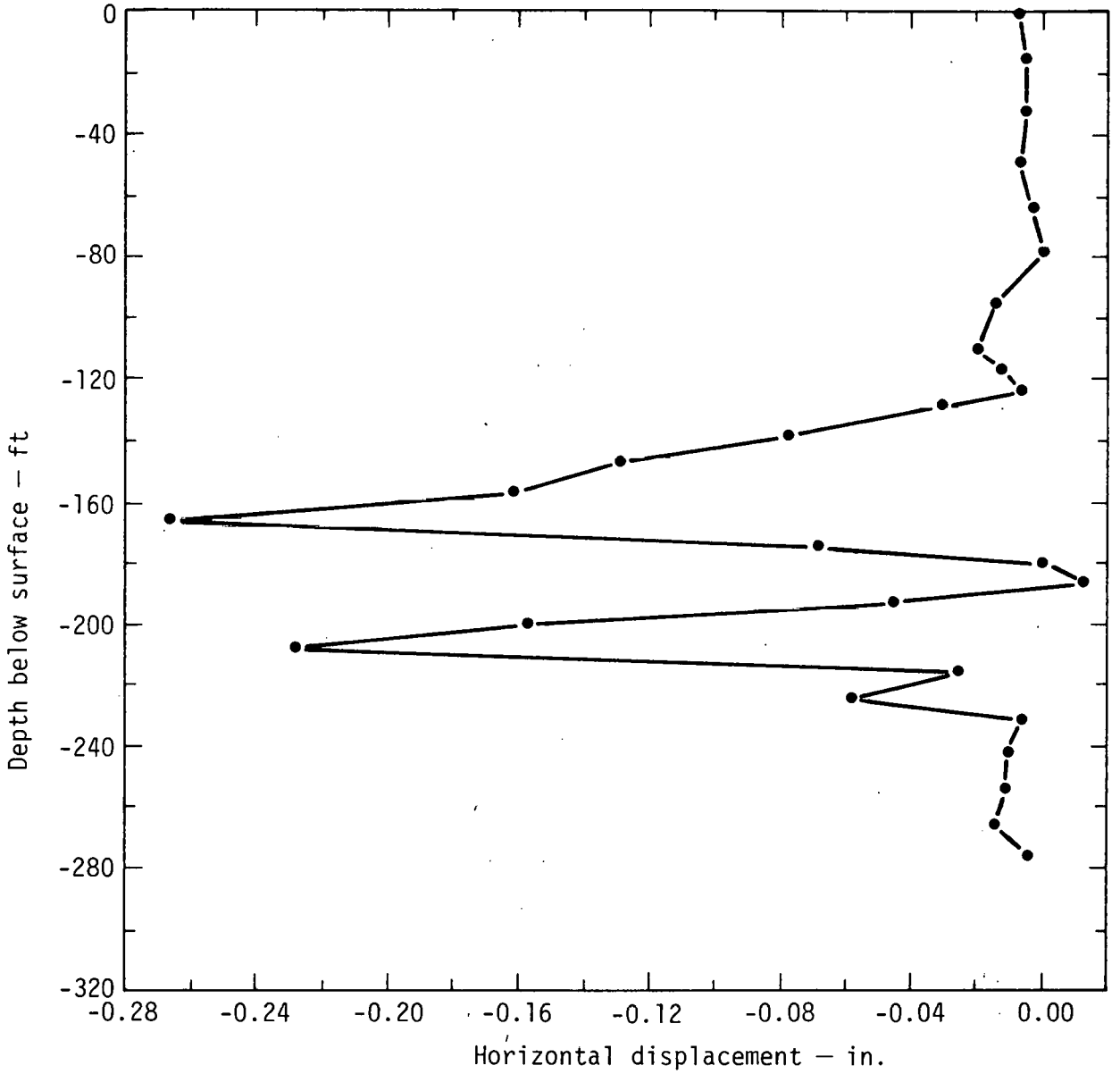

Fig. 12. Horizontal displacement vs depth along R = 20.8 ft (stiff model).

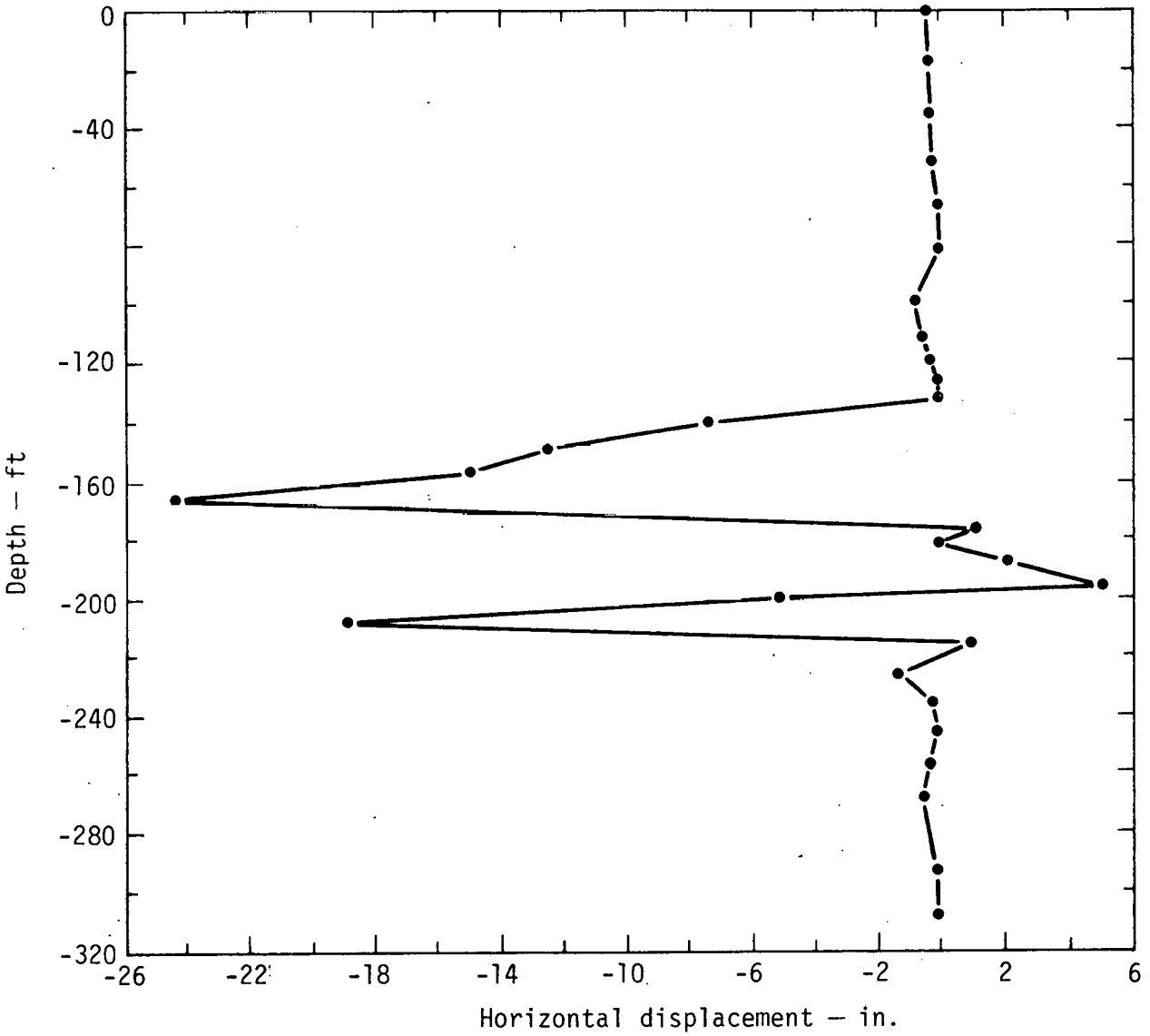

Fig. 13. Horizontal displacement vs depth along R = 20.8 ft (soft model).

Printed in the United States of America
Available from
National Technical Information Service
U.S. Department of Commerce
5285 Port Royal Road
Springfield, VA 22161
Price: Printed Copy $; Microfiche $3.00

Page Range	Domestic Price	Page Range	Domestic Price
001–025	$ 3.50	326–350	10.00
026–050	4.00	351–375	10.50
051–075	4.50	376–400	10.75
076–100	5.00	401–425	11.00
101–125	5.50	426–450	11.75
126–150	6.00	451–475	12.00
151–175	6.75	476–500	12.50
176–200	7.50	501–525	12.75
201–225	7.75	526–550	13.00
226–250	8.00	551–575	13.50
251–275	9.00	576–600	13.75
276–300	9.25	601–up	*
301–325	9.75		

*Add $2.50 for each additional 100 page increment from 601 to 1,000 pages; add $4.50 for each additional 100 page increment over 1,000 pages.

Technical Information Department
LAWRENCE LIVERMORE LABORATORY
University of California | Livermore, California | 94550